Potential Predictability of Seasonal Extreme Precipitation Accumulation in China

WENGUANG WEI AND ZHONGWEI YAN

Key Laboratory of Regional Climate–Environment for Temperate East Asia, Institute of Atmospheric Physics, Chinese Academy of Sciences, and University of Chinese Academy of Sciences, Beijing, China

P. D. JONES

Climatic Research Unit, School of Environmental Sciences, University of East Anglia, Norwich, United Kingdom, and Center of Excellence for Climate Change Research, Department of Meteorology, King Abdulaziz University, Jeddah, Saudi Arabia

(Manuscript received 17 June 2016, in final form 12 December 2016)

ABSTRACT

The potential predictability of seasonal extreme precipitation accumulation (SEPA) across mainland China is evaluated, based on daily precipitation observations during 1960–2013 at 675 stations. The potential predictability value (PPV) of SEPA is calculated for each station by decomposing the observed SEPA variance into a part associated with stochastic daily rainfall variability and another part associated with longer-time-scale climate processes. A Markov chain model is constructed for each station and a Monte Carlo simulation is applied to estimate the stochastic part of the variance. The results suggest that there are more potentially predictable regions for summer than for the other seasons, especially over southern China, the Yangtze River valley, the north China plain, and northwestern China. There are also regions of large PPVs in southern China for autumn and winter and in northwestern China for spring. The SEPA series for the regions of large PPVs are deemed not entirely stochastic, either with long-term trends (e.g., increasing trends in inland northwestern China) or significant correlation with well-known large-scale climate processes (e.g., East Asian winter monsoon for southern China in winter and El Niño for the Yangtze River valley in summer). This fact not only verifies the claim that the regions have potential predictability but also facilitates predictive studies of the regional extreme precipitation associated with large-scale climate processes.

1. Introduction

Influenced by the East Asian monsoon together with other climate factors, China experiences large variability of precipitation, especially for the summer season. Subregional differences of variability of seasonal precipitation are also notable because of the complex geography and extensive range of the country. Many weather systems can bring extreme precipitation to China (Luo et al. 2016), including tropical cyclones, surface fronts, vortex/shear lines, and other small-scale synoptic systems. Disastrous extreme precipitation events occasionally occur across the country due to these stochastic weather phenomena. However, the size of some events has been of increasing concern in recent decades. Examples include the extreme rains throughout almost the whole country during the summer of 1998 (Zong and Chen 2000) and the extreme snowfall/cold rains in southern China in early spring of 2008 (Wang et al. 2008; Gao et al. 2008), which caused huge economic losses and damages to human society. Efforts have been made to uncover the intrinsic characteristics of interannual variability in seasonal precipitation, to ascribe regional precipitation variability to large-scale factors (e.g., sea surface temperature anomalies) that are potentially more predictable, and to improve the seasonal precipitation prediction skill of current models (Wang et al. 2005; Wu et al. 2009; Tian and Fan 2012; Deng et al. 2014; Li et al. 2015).

However, it remains unclear how much seasonal precipitation can be predicted, especially for the extreme events. With regard to the disastrous events, it is

Corresponding author e-mail: Zhongwei Yan, yzw@tea.ac.cn

DOI: 10.1175/JHM-D-16-0141.1

the extreme part of precipitation that matters more directly than seasonal total precipitation. Notably, there have been studies showing that for some well-known climatic teleconnections (e.g., more summer rainfall in the Yangtze River valley in eastern China corresponding to warmer sea surface temperature in the tropical eastern Pacific or El Niño in the preceding winter), the extreme rains play a key role while lighter rains do not contribute to the teleconnections at all (Wang and Yan 2011). It is therefore implied that the extreme part of seasonal precipitation could be more predictable for particular regions, though the general prediction of seasonal precipitation totals over the East Asian monsoon regions remains challenging.

The so-called potential predictability (PP) usually denotes a specific signal-to-noise ratio of variability in seasonal precipitation totals (Madden 1976; Leith 1978; Trenberth 1984). It is thought that observed variability in seasonal precipitation arises partly or totally from high-frequency weather fluctuations (daily precipitation processes), which are unpredictable beyond a few days. Alternatively, variability may result from slowly changing climate processes (e.g., El Niño–Southern Oscillation, continental snow cover and sea ice distributions, and land–atmosphere interaction), which are potentially predictable at longer time scales (Lorenz 1973; Leith 1973; Madden 1976; Madden and Shea 1978; Leith 1978; Somerville 1987; DelSole and Tippett 2007). In past years, there have been a number of studies assessing the PP of seasonal precipitation totals in China (Wang et al. 1997; Liu et al. 2000; Ying et al. 2013). There also have been a few studies about PP of seasonal extreme precipitation but for other non-Chinese regions (Becker et al. 2013; Anderson et al. 2015). It is beneficial to have a general assessment of PP for extreme precipitation in mainland China.

The present work extends the PP analysis to seasonal extreme precipitation accumulation (SEPA) over mainland China for the first time. SEPA is defined as the sum of all daily precipitation totals beyond the 95th percentile (R95) in the season (referred to as R95pTOT). This is one of the extreme precipitation indices recommended by ETCCDI (Klein Tank et al. 2009; Zhang et al. 2011). This index represents the portion of seasonal extreme precipitation that could possibly result in disastrous events (e.g., urban waterlogging, landslide, and flooding). This paper seeks to demonstrate the regions of significant PP of SEPA for different seasons by applying a recently improved chain-dependent Markov process with a variable order for each day of the year to simulate the weather noise (Gianotti et al. 2013, 2014; Anderson et al. 2015). Furthermore, the present paper's aims are to explain possible sources of the potential predictability of SEPA in the regions with large PP values in order to further verify the potential predictability in these regions. The data and methods used are explained in section 2. The results are demonstrated in section 3. Conclusions with discussion are summarized in section 4.

2. Data and methods

a. Data

A set of daily precipitation data at 824 stations in China was obtained from the Chinese Meteorological Information Center. We select a subset of 675 stations without missing data between 1 January 1960 and 31 December 2013. Most of the country is well covered except for parts of the Tibetan Plateau and western Inner Mongolia.

To calculate the SEPA for each day, we estimate for each calendar day a base cumulative distribution function (CDF) by using all daily records of nonzero daily precipitation amounts within a 91-day window (centered around the given calendar day) during 1960–2013 and then calculate the 95th percentile as a threshold to calculate the daily SEPA. In cases without any daily precipitation records exceeding the threshold within the season (a 91-day window), SEPA is defined as the maximum daily precipitation amount during the 91-day period for these years, in order to avoid a discontinuity of the time series. For convenience, the SEPA series for each station starts from 1 March 1960 to 28 February 2013 (omitting 29 February for leap years), thus being 53 years in length.

The 3-month running mean of sea surface temperature anomaly (SSTA) for the Niño-3.4 region is obtained from the NOAA/Climate Prediction Center and an El Niño (La Niña) event is defined by a minimum of five consecutive overlapping seasons with SSTA above 0.5°C (below −0.5°C). An East Asian winter monsoon (EAWM) index defined by Wang and Chen (2014) is also used in the subsequent analysis.

b. Methods

To determine the bounds of variability generated by stochastic short-term processes in the SEPA series, we apply a recently improved method (Gianotti et al. 2013, 2014; Anderson et al. 2015) by using a stationary stochastic process to model the occurrence and intensity of daily precipitation events. In this method, a chain-dependent Markov process is used to simulate the occurrence process. For the present study, such stochastic processes should ideally describe the statistical characteristics of stochastic short-term daily weather events, but cannot explain variability generated by

longer-time-scale climate processes. For each station, we build a model of daily varying order but interannually stationary Markov chain with all parameters estimated from the historical records to simulate the occurrence of daily precipitation events. Specifically, in this model, every day of the year possesses an order between 0 and 3 selected by the corrected Akaike information criterion (AICc; Hurvich and Tsai 1989). To guarantee a robust estimate of a day's parameters (order and the corresponding transition probabilities) in the chain, the historical data within a certain number of neighboring days (between 5 and 91 days also determined via AICc) are selected as samples for that day.

In this stationary stochastic model, the occurrence process is accompanied with an intensity process also representing the variability attributed to high-frequency weather noise in precipitation intensity. Previous studies have reported that the precipitation intensity on a day might have some correlation with the precipitation occurrence or intensity on the previous days (Wilks 1999). Having assessed this in the study region of mainland China, we construct an intensity process model with a continuous parametric density function conditioned on the previous m days' precipitation states. Here, the number of previous days m is selected from 0 to 3 via AICc. The probability density function (PDF) of nonzero precipitation intensity was supposed to follow a mixed gamma distribution. This PDF was selected after comparing with several other PDFs used in previous studies (e.g., gamma, exponential, and mixed exponential; Wilks 1999; Anderson et al. 2015), with regard to their ability to represent the tail of the distribution of daily precipitation amounts. The mixed gamma takes the form as follows:

$$f(x) = \frac{a}{\Gamma(\alpha_1)\beta_1^{\alpha_1}} x^{\alpha_1 - 1} \exp\left(-\frac{x}{\beta_1}\right) + \frac{(1-a)}{\Gamma(\alpha_2)\beta_2^{\alpha_2}} x^{\alpha_2 - 1} \exp\left(-\frac{x}{\beta_2}\right), \quad x > 0,$$

where x represents the amount of daily precipitation, $0 < a < 1$ and α_1, β_1, α_2, $\beta_2 > 0$. The five parameters of the mixed gamma distribution function for each day are estimated from samples constructed by pooling the data within a 91-day window centered on that day to enhance the robustness of estimates. The choice of a 91-day window is beneficial, especially for arid regions where precipitation days are very few.

With the occurrence model and intensity model both built, the daily-varying-order, yearly stationary stochastic weather model is complete. For each station, we use this model to produce 1000 Monte Carlo simulations for 53 years, the same length as the historical series. Based on the observed records and the 1000 simulations, the potential predictability for a certain day is defined as

$$\mathrm{PP}(d) = \frac{\sigma^2_{\mathrm{obs}}(d) - \overline{\sigma^2_{\mathrm{sim}}(d)}}{\sigma^2_{\mathrm{obs}}(d)},$$

where PP is the estimated potential predictability value (PPV), d is the day of year, σ^2_{obs} is the observed variance of R95pTOT for the day, and $\overline{\sigma^2_{\mathrm{sim}}}$ is the mean simulated variance (averaged from the 1000 simulated variances). By definition, the potential predictability can be seen as the fraction of variance produced by low-frequency processes.

To test the statistical significance of any potential predictability, we need to estimate the CDF of PP under the null hypothesis that there is no potential predictability. This is accomplished by defining simulated PP as follows:

$$\mathrm{PP}_{\mathrm{sim}}(n,d) = \frac{\sigma^2_{\mathrm{sim}}(n,d) - \overline{\sigma^2_{\mathrm{sim}}(d)}}{\sigma^2_{\mathrm{sim}}(n,d)}, \quad n = 1,\ldots,1000,$$

where $\sigma^2_{\mathrm{sim}}(n, d)$ is the variance in the nth run. Since every run of the stochastic model is under the condition of no potential predictability, $\mathrm{PP}_{\mathrm{sim}}(n, d)$ defined above can be seen as a sample under the null hypothesis. Hence, the 1000 samples allow an estimate of the CDF of PP to be made under the null hypothesis. If the observed PP is larger than the criterion given the significance level of 0.1, the null hypothesis is rejected, that is, there is significant potential predictability for the day.

As an example, Fig. 1 illustrates the annual cycle of PPV with the corresponding confidence interval at one station (Fig. 1). In Fig. 1, the shaded area represents the likely range of the stochastic-weather-induced variability. The wide range of the confidence interval indicates large uncertainty resulting from weather noise. However, the PPV for this station is well above the stochastic range throughout the summer, indicating significant PP for summer at this station. In the case where the PPV is smaller than the mean simulated PPV (e.g., at the end of February and the beginning of March for this station), a negative PPV is obtained. The interpretation of a negative PPV will be discussed in the last section. As the present paper focuses on the cases of extra variability beyond weather noise, the occasional negative PP values will be omitted in the subsequent analysis.

Although the PPV for any given day of the year can be calculated, the present paper mainly discusses the results corresponding to the traditional four seasons, that is, those around the 46th day (15 April) in the annual cycle for spring, the 137th day (15 July) for summer, the 229th day (15 October) for autumn, and the 321st day (15 January) for winter. The time of the maximum PPV during the year is also analyzed for each station and

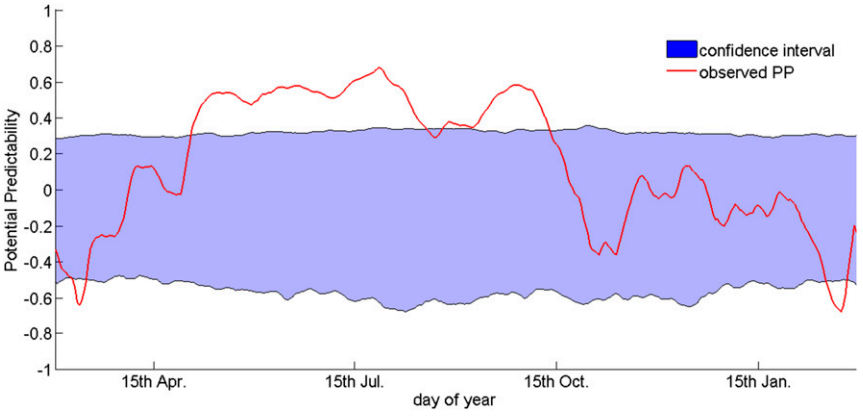

FIG. 1. The PP of SEPA (R95pTOT) on each day of the year for Shaoyang station (Hunan Province).

categorized into one of the four traditional seasons. To facilitate identifying the large-scale patterns of high/low PPVs, we interpolate the station results onto 0.1° × 0.1° grids by using Kernel density estimation.

3. Results

a. Potential predictability of SEPA

In general, small PPVs prevail throughout the country for all seasons (Fig. 2), implying that it is difficult to predict the extreme part of seasonal precipitation. However, all stations with statistically significant PPVs have a PPV larger than 0.3, and there are a few subregions with large PPVs for a season. Summer shows most subregions with large PPVs among the four seasons, as shown in JJA in Fig. 2. The regions of statistically significant PP for summer extend quite broadly, including a large part of northern China (from Xinjiang to northeastern China), the middle to lower reaches of the Yangtze River and Huai River, the north China plain, and southern China. There are several large areas with little PP, including southwestern China and the Gulf of Bohai, while statistically insignificant PPVs also scatter elsewhere.

For autumn, the predictable areas diminish obviously (Fig. 2, SON). There is a widespread zone with little PP extending from the eastern Tibetan Plateau

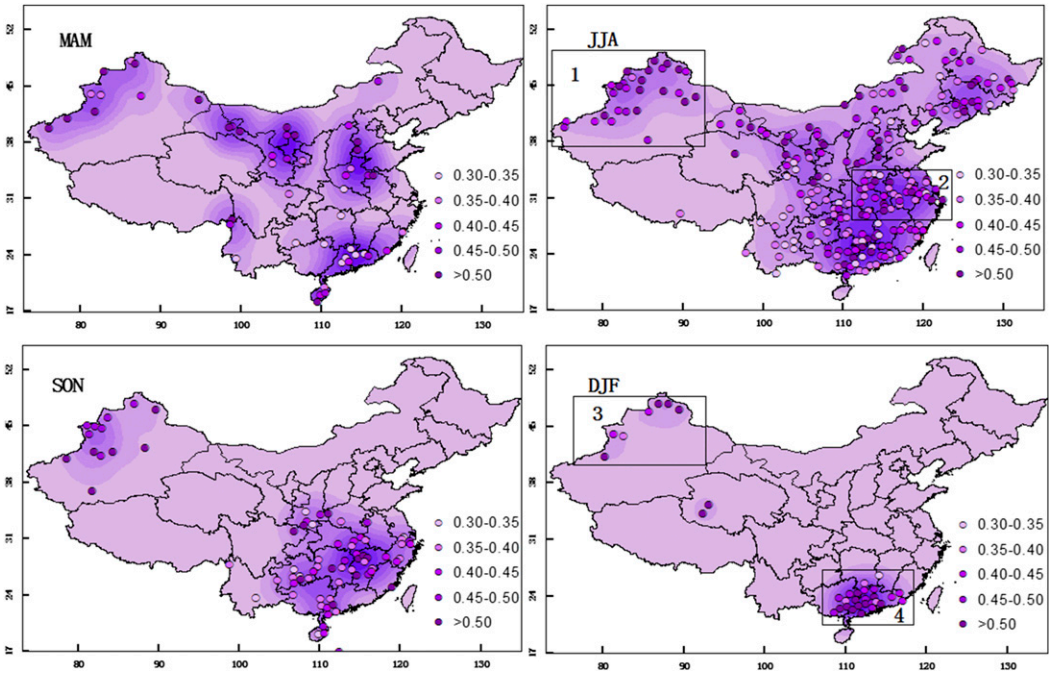

FIG. 2. Distribution of PP in SEPA (R95pTOT) for the four seasons.

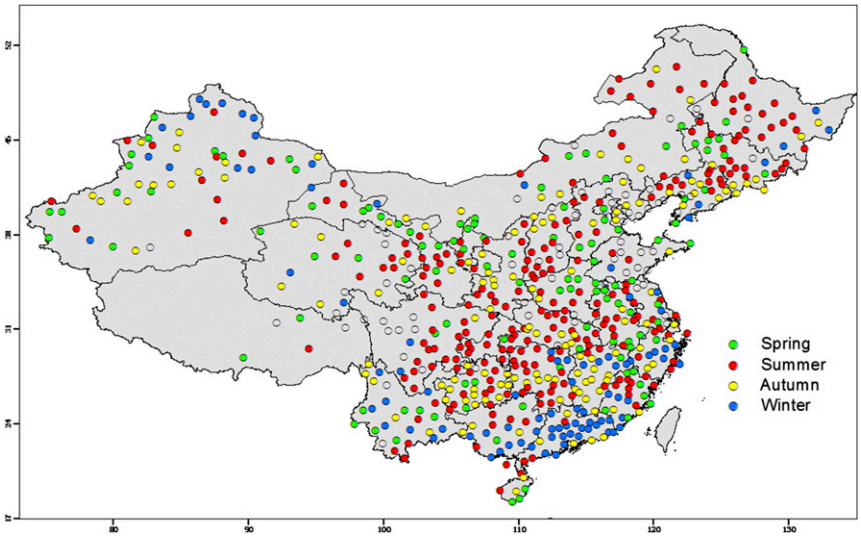

FIG. 3. Spatial distribution of max PP time (into the four seasons).

to northeastern China. There are several relatively large regions with PPV $\geq$ 0.3, including western Xinjiang, southern Shaanxi, parts of Hunan and Jiangxi, and southern Guangdong.

For winter, the area with little PP further expands to cover most of China (Fig. 2, DJF). In contrast, the predictable area in southern China is enlarged. Large PPVs also exist in the extreme northwest of China, around the northern Junggar basin.

For spring, the highest PPVs are found over western Xinjiang, Ningxia, and the north China plain. Statistically significant PPVs also exist around Hainan Island and coastal southern China (Fig. 2, MAM).

To help summarize the results of Fig. 2, we calculate the maximum PPV during the year for each station and see in which season it occurs (Fig. 3). From the map of the maximum PPV time, we can see that some stations in the eastern Tibetan Plateau, the Gulf of Bohai, and Shandong Peninsula have no PP for SEPA throughout the year. Large areas in central and northern China have a maximum PP in summer, especially including the middle to lower reaches of the Yangtze River, eastern Sichuan basin, and northeastern China. The regions with the maximum PP time in autumn are mainly located in southern China and middle Xinjiang. Northern Xinjiang and Guangdong are the only two regions with their maximum PP time in winter. The southern part of the north China plain and some small parts in northern China show the maximum PP in spring.

b. Sources of potential predictability

The regions with a number of stations where the variability of SEPA is beyond simulated weather noise should experience some nonstationary processes. Such nonstationary processes possibly result either from some long-term internal climate dynamics or external forcings for the regions, which renders the SEPA potentially predictable and could be regarded as the sources of PP.

Four specific regions (as marked in Fig. 2) are selected to investigate possible causes of the large PPVs. To see whether there are some common sources of potential predictability in the aggregated stations with high PPVs and to dampen the noise from individual station series, we calculate regional-mean R95pTOT series by using all stations with PPV $\geq$ 0.3 within the selected region.

Three of the selected regions show statistically significant trends, including Xinjiang for summer (region 1 in Fig. 2), northern Xinjiang for winter (region 3 in Fig. 2), and the middle to lower reaches of the Yangtze River for summer (region 2 in Fig. 2). The increasing rates of the three regional R95pTOT series are 0.193, 0.209, and 1.187 mm yr^{-1} (Fig. 4) and the coefficients of determination are 20.2%, 16.3%, and 9.1%, respectively. Considering the averaged PP over these three regions are 0.5 (Xinjiang for summer), 0.53 (northern Xinjiang for winter), and 0.45 (the middle to lower reaches of the Yangtze River for summer), the contributions of the linear trend to the potential predictability are 40%, 30%, and 20%, respectively (Table 1). Although these cannot account for all the potential predictability for the regions, the long-term trend is indeed an obvious source for nonstationarity of a time series, and there is usually a driving process behind it (e.g., global warming and transition from one to another phase of some large-scale climate oscillation). For Xinjiang in northwestern China, previous studies

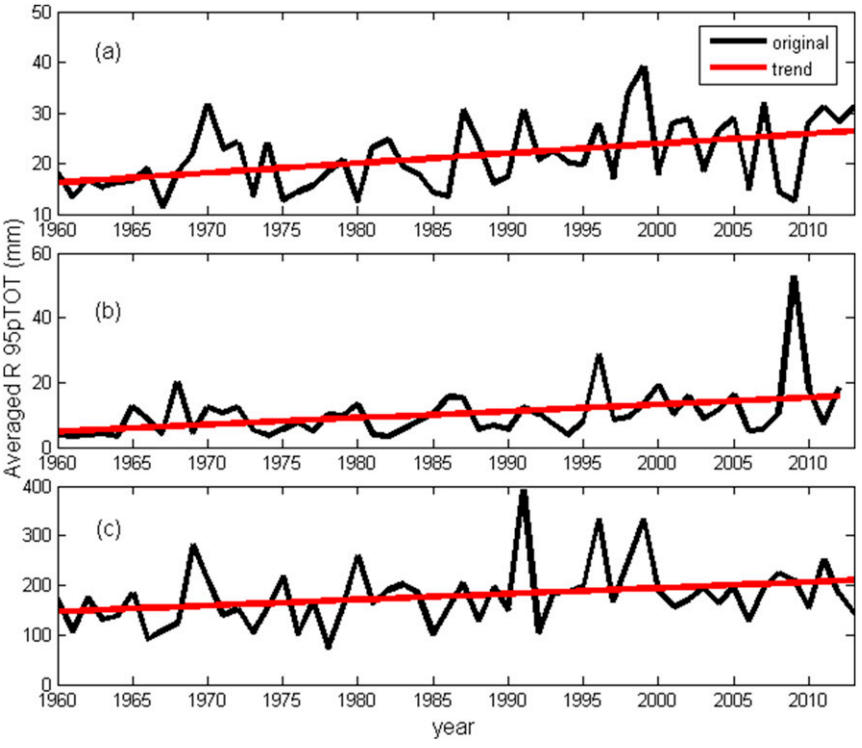

FIG. 4. Three regional R95pTOT series with high PPVs partly due to a statistically significant increasing trend.

have shown that, during the past half century, increasing atmospheric water vapor mainly comes from the North Atlantic and the Arctic Ocean for summer and from the Caspian Sea and the Mediterranean for winter (Dai et al. 2007). A major increase of the water vapor in Xinjiang happened in the middle of the 1980s. This regional wetting trend has been ascribed to the effect of significant climate warming in middle and high latitudes during the same period (Dai et al. 2007; Sun and Ao 2013). Such a wetting trend supports the increasing trend in the extreme part of precipitation, contributing to some PP of SEPA (R95pTOT) over the region. For the Yangtze River region, there also have been many studies showing that both the summer total precipitation and extreme precipitation have been increasing during the last few decades (Su et al. 2006; Wang and Zhou 2005).

Besides the long-term trends, there should be more sources of potential predictability for the regional SEPA in association with large-scale climate processes. The winter SEPA of southern China (region 4 in Fig. 2) serves as an example. It is noted that most of the stations in this region consistently observe higher values of SEPA in some years and much less in some other years. Averaging of all correlation coefficients between each individual series and the regional average, we get a mean correlation of 0.81, indicating strongly consistent variations in the SEPA series (Fig. 5a). This is an indicator of the existence of some large-scale climate variations. The correlation analysis between SEPA and some large-scale climate processes discovered that the EAWM has significant connection with the winter regional SEPA over southern China (Fig. 5b), and the regression result shows that EAWM accounts for 14% of the regional SEPA interannual variability and 35.9% of the regional-mean PP (Table 1). Therefore, it is reasonable to regard

TABLE 1. Regression between regional SEPA and some sources of PP (e.g., long-term trends and EAWM). The numbers after "SEPA" in the first column represent the marked four regions in Fig. 2. The coefficient of determination for the regression is given by R^2, representing how much variability the regression can account from the total variability. The ratio of R^2 to the regional-mean PP represents the portion of PP the regression could account for.

Regression form	R^2	P value (F test)	Regional mean PP	Ratio (R^2/PP)
SEPA(1)–year	0.20	0.0006	0.50	40%
SEPA(2)–year	0.09	0.03	0.45	20%
SEPA(3)–year	0.16	0.003	0.53	30%
SEPA(4)–EAWM	0.14	0.005	0.39	36%

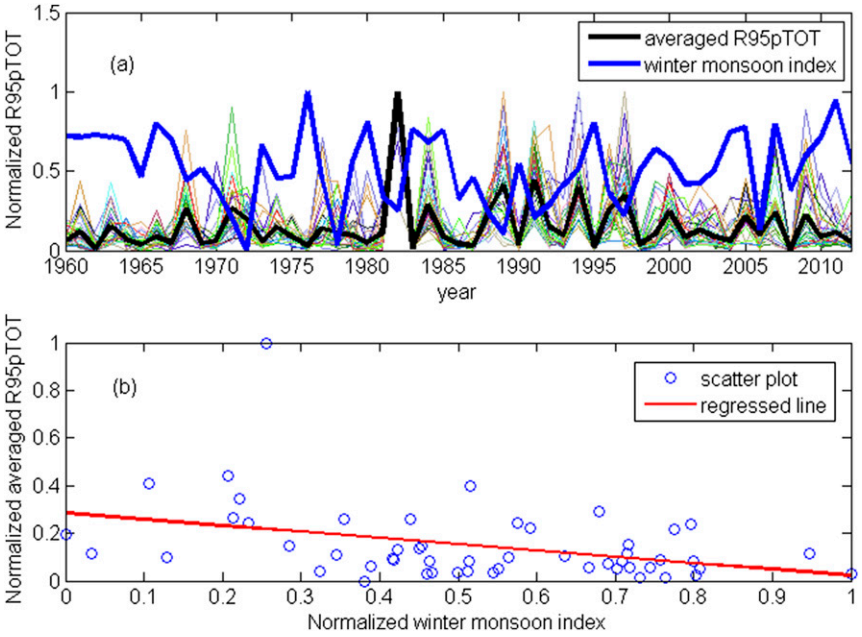

FIG. 5. Correlation between winter SEPA over southern China and the winter monsoon index.

EAWM as a source of potential predictability in extreme precipitation over this region for winter.

As for the middle to lower reaches of the Yangtze River (region 2 in Fig. 2) for summer, the observed trend during the past half century is a possible cause, but seasonal rainfall observations have also been shown to be associated with some long-term climate processes such as ENSO, the Pacific decadal oscillation (PDO), the subtropical northwestern Pacific high (SNPH), and the East Asian summer monsoon (EASM; Gong and Ho 2002; Zhu and Yang 2003; Wu et al. 2009; Zong et al. 2010; Wang and Yan 2011). It is difficult to determine a steady and simple relationship between the regional summer SEPA and any one of these large-scale factors, because the variability of SEPA arises from the combination of effects of these processes. In spite of this, the influence of some climate processes on the regional summer SEPA series can still be identified. In particular, it is notable that 5 out of 7 years with the detrended regional SEPA exceeding one standard deviation σ were summers following El Niño events. This indicates El Niño as a possible factor for this region that leads to more extreme rains in summer (Fig. 6). Some studies also found that the EASM has a negative correlation with extreme precipitation in this region (Wang and Yan 2011). It is clear that precipitation over this region is not determined by only a single large-scale climate factor but depends on interactions among several climate processes. These processes make it complicated to predict the seasonal precipitation for this region, even with considerable PP.

For the other regions with large PPVs (e.g., western Xinjiang in spring and northeastern China in summer), the regional R95pTOT series also demonstrates some nonrandomness that might arise from consistent variations of SEPA for most of the stations in the region. Such consistent behavior is beyond the variations from stochastic weather processes, and the spatial agreement implies it must be related to some longer-term climate processes.

In contrast, the stations within regions of insignificant PPVs do not show such characteristics. The seasonal R95pTOT series in those regions can be regarded mainly as stochastic weather noise. For example, for the eastern edge of Tibetan Plateau for summer, many stations are found to have statistically insignificant PPVs while the R95pTOT series at each station is found to be barely above the noise level. For these regions, most of the stations do not show consistent variations in SEPA for any years. As a result of this, the regional-mean R95pTOT series is also identified as noise, that is, hardly predictable.

4. Summary and discussion

In this paper, the PP of seasonal extreme precipitation accumulation over mainland China is evaluated. We constructed stationary stochastic weather models based on instrumental station records and estimate the variance of SEPA associated with stochastic short-term daily weather fluctuations by using Monte Carlo simulations for each station and day of the year. The PPV is defined as

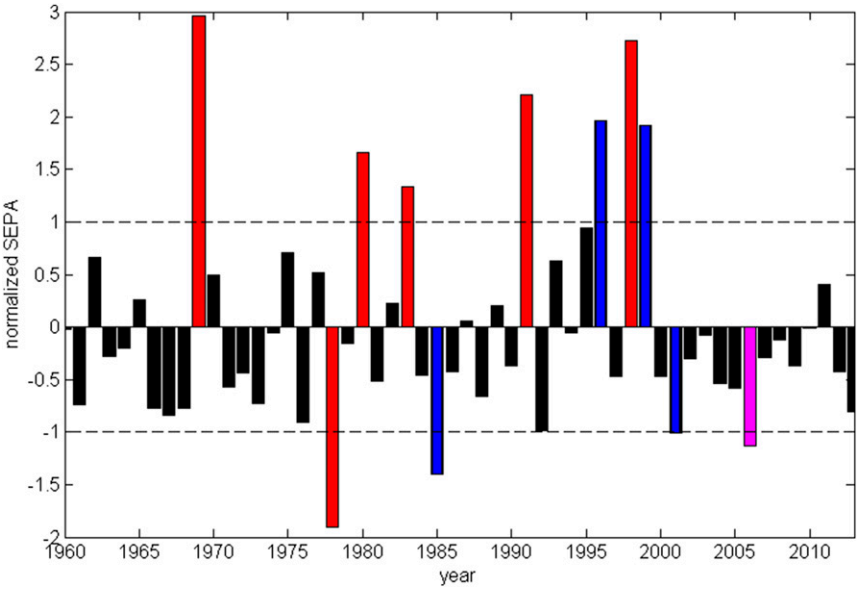

FIG. 6. Detrended regional SEPA over the middle to lower reaches of the Yangtze River for summer.

the fraction of the observed variance after removing the stochastic part. Based on the PPVs at all stations over mainland China, the distribution of PP for seasonal precipitation extremes can be visualized for each day of the year. Focusing on PP for the conventional four seasons, we found typical regions with high PPVs and the analysis of the SEPA time series for each station verified the existence of potential predictability in stations within the typical regions. Main conclusions are as follows.

1) Overall, for summer, western Xinjiang, the middle to lower reaches of the Yangtze and Huai Rivers, the Sichuan basin, northeastern China, and southern China are the regions with consistently large PPVs $\geq$0.3 at most stations. For autumn, the predictable regions greatly reduce, with only small regions in Xinjiang and the middle and south of China having PPV $\geq$ 0.3. For winter, a large part of southern China and northern Xinjiang exhibit high PPVs. For spring, there are few predictable regions, except for western Xinjiang. Most regions have their maximum PP time in summer, especially for central and northern China.
2) The regional SEPA (or R95pTOT) series for the typical regions with high PPVs do show some types of nonstationarity or nonrandomness, which verifies our claim of potential predictability there. A common feature of the R95pTOT series for these regions is that many stations have PPVs $\geq$0.3 within a region showing consistent variations in SEPA, resulting in some years with consistently more (or less) SEPA throughout the region. The middle to lower reaches of the Yangtze River and Xinjiang for summer and northern Xinjiang for winter exhibited statistically significant long-term increasing trends in SEPA during the past half century. The regional winter R95pTOT series over southern China showed statistically significant correlation with the EAWM index, suggesting a strong influence of the EAWM on SEPA in this region. The regional summer SEPA in the middle to lower reaches of the Yangtze River was large in most of the summers following El Niño. All of these examples imply that some large-scale climate processes drive the regional extreme precipitation beyond the local weather noise, thus rendering the regional SEPA potentially predictable. In contrast, the regions with no PP should be influenced more by stationary stochastic weather noise.

It is noteworthy that there have been few studies about the potential predictability in seasonal extreme precipitation over the East Asian monsoon region. The present paper provides the first attempt to evaluate the PP of SEPA in China. Note that a PPV of 0.3 means that 30% of the total variance results from potentially predictable signals while 70% should be from noise. Except for the typical regions outlined in our study, most of China exhibited PPVs smaller than 0.3 in general, which means that weather noise is dominant in the SEPA variability in general. This poses a serious challenge for prediction of SEPA for the regions.

Caveats for understanding the present results also arise from the imperfect models. For instance, the 95th

percentile of daily precipitation tends to be overestimated at some stations for the dry season (e.g., winter) by the model, which should influence the subsequent PP analysis. We have checked that the number of wet days for each station is well simulated for all seasons by the model. This implies that the occurrence process model is sufficiently good and the biased 95th percentiles of daily precipitation are likely caused by the intensity process simulation. In fact, the observed distribution of daily precipitation totals for the dry season usually contains a considerable number of light rain days and several heavy rain days, but few moderate rain days. As a result of this, the empirical 95th percentile tends to be smaller than that of a fitted theoretical distribution. Unfortunately, there is not a perfect model that fits daily precipitation well for all seasons and stations across a large region such as China.

A remaining problem is about the emergence of the negative PP. There are 13% of the stations showing negative PP and with poorly fitted R95 by the model, mostly for winter. The failure of the model to represent the observed distribution of daily precipitation for the dry season is a likely cause. For those where the model reproduces R95 well but also shows a negative PP (1%), an alternative explanation is that some long-term climate processes suppress the weather-induced stochastic variability.

Another shortcoming of the current method is that the stationary stochastic weather model does not describe any spatial dependence of weather variability among the stations. A more perfect model with improvements toward this shortcoming helps to obtain more reliable assessments of the potential predictability.

Nevertheless, it is interesting to note that a large part of China shows some consistent PP for summer SEPA, which, in association with the EASM, has long been a target of research in the field of climatology. In contrast, the predictive skill of current predictive models for seasonal precipitation totals remains low for this region (Wang et al. 2009, 2015). This implies considerable potential for the improvement of current predictive models. To realize this, it is beneficial to further study the underlying large-scale climate processes and the relevant mechanisms leading to extreme precipitation in the region. Knowing the possible sources of potential predictability for typical regions should help to facilitate development of relevant modeling studies and predictive methods.

Acknowledgments. This study was supported by the National Basic Research Program of China (Grant 2016YFA0600400) and Chinese Academy of Sciences International Collaboration Program (2016) both to Zhongwei Yan.

REFERENCES

Anderson, T. B., D. J. Gianotti, and G. D. Salvucci, 2015: Characterizing the potential predictability of seasonal, station-based heavy precipitation accumulations and extreme dry spell durations. *J. Hydrometeor.*, **16**, 843–856, doi:10.1175/JHM-D-14-0111.1.

Becker, E. J., H. van den Dool, and M. Peña, 2013: Short-term climate extremes: Prediction skill and predictability. *J. Climate*, **26**, 512–531, doi:10.1175/JCLI-D-12-00177.1.

Dai, X. G., W. J. Li, Z. G. Ma, and P. Wang, 2007: Water-vapor source shift of Xinjiang region during the recent twenty years. *Prog. Nat. Sci.*, **17**, 569–575, doi:10.1080/10020070708541037.

DelSole, T., and M. Tippett, 2007: Predictability: Recent insights from information theory. *Rev. Geophys.*, **45**, RG4002, doi:10.1029/2006RG000202.

Deng, Y. Y., T. Gao, H. W. Gao, X. H. Yao, and L. Xie, 2014: Regional precipitation variability in East Asia related to climate and environmental factors during 1979–2012. *Sci. Rep.*, **4**, 5693, doi:10.1038/srep05693.

Gao, H., and Coauthors, 2008: Analysis of the severe cold surge, ice-snow and frozen disasters in south China during January 2008: II. Possible climatic causes (in Chinese). *Meteor. Mon.*, **34** (4), 101–106.

Gianotti, D. J., B. T. Anderson, and G. D. Salvucci, 2013: What do rain gauges tell us about the limits of precipitation predictability? *J. Climate*, **26**, 5682–5688, doi:10.1175/JCLI-D-12-00718.1.

——, ——, and ——, 2014: The potential predictability of precipitation occurrence, intensity, and seasonal totals over the continental United States. *J. Climate*, **27**, 6904–6918, doi:10.1175/JCLI-D-13-00695.1.

Gong, D. Y., and C. H. Ho, 2002: Shift in the summer rainfall over the Yangtze River valley in the late 1970s. *Geophys. Res. Lett.*, **29**, 1436, doi:10.1029/2001GL014523.

Hurvich, C. M., and C. L. Tsai, 1989: Regression and time series model selection in small samples. *Biometrika*, **76**, 297–307, doi:10.1093/biomet/76.2.297.

Klein Tank, A. M. G., F. W. Zwiers, and X. Zhang, 2009: Guidelines on analysis of extremes in a changing climate in support of informed decisions for adaptation. WCDMP-72, WMO/TD-1500, 56 pp. [Available online at www.wmo.int/datastat/documents/WCDMP_72_TD_1500_en_1_1.pdf.]

Leith, C. E., 1973: The standard error of time-average estimates of climatic means. *J. Appl. Meteor.*, **12**, 1066–1069, doi:10.1175/1520-0450(1973)012<1066:TSEOTA>2.0.CO;2.

——, 1978: Predictability of climate. *Nature*, **276**, 352–355, doi:10.1038/276352a0.

Li, Z. X., T. J. Zhou, H. S. Chen, D. H. Ni, and R. H. Zhang, 2015: Modeling the effect of soil moisture variability on summer precipitation variability over East Asia. *Int. J. Climatol.*, **35**, 879–887, doi:10.1002/joc.4023.

Liu, Y. J., K. Y. Ma, and Z. S. Lin, 2000: Potential predictability of monthly precipitation over China. *Acta Meteor. Sin.*, **14** (3), 316–329.

Lorenz, E. N., 1973: Predictability and periodicity: A review and extension. *Proc. Third Conf. on Predictability and Statistics in the Atmospheric Sciences*, Boulder, CO, Amer. Meteor. Soc., 1–4.

Luo, Y. L., M. W. Wu, F. M. Ren, J. Li, and W. K. Wong, 2016: Synoptic situations of extreme hourly precipitation over China. *J. Climate*, **29**, 8703–8719, doi:10.1175/JCLI-D-16-0057.1.

Madden, R. A., 1976: Estimates of the natural variability of time averaged sea level pressure. *Mon. Wea. Rev.*, **104**, 942–952, doi:10.1175/1520-0493(1976)104<0942:EOTNVO>2.0.CO;2.

——, and D. Shea, 1978: Estimates of the natural variability of time-averaged temperatures over the United States. *Mon. Wea. Rev.*, **106**, 1695–1703, doi:10.1175/1520-0493(1978)106<1695:EOTNVO>2.0.CO;2.

Somerville, R., 1987: The predictability of weather and climate. *Climatic Change*, **11**, 239–246, doi:10.1007/BF00138802.

Su, B. D., T. Jiang, and W. B. Jin, 2006: Recent trends in observed temperature and precipitation extremes in the Yangtze River basin, China. *Theor. Appl. Climatol.*, **83**, 139–151, doi:10.1007/s00704-005-0139-y.

Sun, J. Q., and J. Ao, 2013: Changes in precipitation and extreme precipitation in a warming environment in China. *Chin. Sci. Bull.*, **58**, 1395, doi:10.1007/s11434-012-5542-z.

Tian, B. Q., and K. Fan, 2012: Relationship between the late spring NAO and summer extreme precipitation frequency in the middle and lower reaches of the Yangtze River. *Atmos. Ocean. Sci. Lett.*, **5**, 455–460.

Trenberth, K. E., 1984: Some effects of finite sample size and persistence on meteorological statistics. Part II: Potential predictability. *Mon. Wea. Rev.*, **112**, 2369–2379, doi:10.1175/1520-0493(1984)112<2369:SEOFSS>2.0.CO;2.

Wang, B., Q. H. Ding, X. H. Fu, I. S. Kang, K. Jin, J. Shukla, and F. Doblas-Reyes, 2005: Fundamental challenge in simulation and prediction of summer monsoon rainfall. *Geophys. Res. Lett.*, **32**, L15711, doi:10.1029/2005GL022734.

——, and Coauthors, 2009: Advance and prospectus of seasonal prediction: Assessment of the APCC/CliPAS 14-model ensemble retrospective seasonal prediction (1980–2004). *Climate Dyn.*, **33**, 93–117, doi:10.1007/s00382-008-0460-0.

Wang, H. J., F. Xue, and X. Q. Bi, 1997: The interannual variability and predictability in a global climate model. *Adv. Atmos. Sci.*, **14**, 554–562, doi:10.1007/s00376-997-0073-2.

——, and Coauthors, 2015: A review of seasonal climate prediction research in China. *Adv. Atmos. Sci.*, **32**, 149–168, doi:10.1007/s00376-014-0016-7.

Wang, L., and W. Chen, 2014: An intensity index for the East Asian winter monsoon. *J. Climate*, **27**, 2361–2374, doi:10.1175/JCLI-D-13-00086.1.

——, and Coauthors, 2008: Analysis of the severe cold surge, ice-snow and frozen disasters in south China during January 2008: I. Climatic features and its impact (in Chinese). *Meteor. Mon.*, **34** (4), 95–100.

Wang, Y., and Z. W. Yan, 2011: Changes of frequency of summer precipitation extremes over the Yangtze River in association with large-scale oceanic–atmospheric conditions. *Adv. Atmos. Sci.*, **28**, 1118–1128, doi:10.1007/s00376-010-0128-7.

Wang, Y. Q., and L. Zhou, 2005: Observed trends in extreme precipitation events in China during 1961–2001 and the associated changes in large-scale circulation. *Geophys. Res. Lett.*, **32**, L09707, doi:10.1029/2005GL023769.

Wilks, D. S., 1999: Interannual variability and extreme-value characteristics of several stochastic daily precipitation models. *Agric. For. Meteor.*, **93**, 153–169, doi:10.1016/S0168-1923(98)00125-7.

Wu, Z. W., B. Wang, J. P. Li, and F. F. Jin, 2009: An empirical seasonal prediction model of the East Asian summer monsoon using ENSO and NAO. *J. Geophys. Res.*, **114**, D18120, doi:10.1029/2009JD011733.

Ying, K. R., X. G. Zheng, X. W. Quan, and C. S. Frederiksen, 2013: Predictable signals of seasonal precipitation in the Yangtze–Huaihe River valley. *Int. J. Climatol.*, **33**, 3002–3015, doi:10.1002/joc.3644.

Zhang, X., L. Alexander, G. C. Hegerl, P. D. Jones, A. Tank Klein, T. C. Peterson, B. Trewin, and F. W. Zwiers, 2011: Indices for monitoring changes in extremes based on daily temperature and precipitation data. *Wiley Interdiscip. Rev.: Climate Change*, **2**, 851–870, doi:10.1002/wcc.147.

Zhu, Y. M., and X. Q. Yang, 2003: Relationships between Pacific decadal oscillation (PDO) and climate variabilities in China (in Chinese). *Acta Meteor. Sin.*, **61** (6), 641–654.

Zong, H. F., L. T. Chen, and Q. Y. Zhang, 2010: The instability of the interannual relationship between ENSO and the summer rainfall in China (in Chinese). *Chin. J. Atmos. Sci.*, **34** (1), 184–192.

Zong, Y. Q., and X. Q. Chen, 2000: The 1998 flood on the Yangtze, China. *Nat. Hazards*, **22**, 165–184, doi:10.1023/A:1008119805106.